ELSEVIER

Thermochimica Acta 306 (1997) 13–21

thermochimica acta

Investigation of the kinetics of the fluidized bed process for the dehydration of $NdCl_3 \cdot 6H_2O$, $TbCl_3 \cdot 6H_2O$ and $DyCl_3 \cdot 6H_2O$

Johan Sundström[a,*], Vu Van Hong[b]

[a] *Department of Metallurgy – Division of Process Metallurgy, The Royal Institute of Technology, S-100 44 Stockholm, Sweden*
[b] *Department of Rare Earth Metals, Institute of Material Science, Vietnam National Center for Natural Science and Technology Nghia do Tu liem, Hanoi, Vietnam*

Received 6 August 1996; accepted 22 May 1997

Abstract

Dehydration of $NdCl_3 \cdot 6H_2O$, $TbCl_3 \cdot 6H_2O$ and $DyCl_3 \cdot 6H_2O$ was carried out by fluidization in a gas mixture of Ar and HCl. In a series of isothermal experiments the effect of different process parameters was considered. Water vapour pressure of gas leaving the fluidized bed was estimated by using a simple mass balance. It was shown that the rate-limiting step of the overall dehydration process in the fluidized bed is removal of water vapour by a saturated bulk gas flow. However, the saturated gas phase data could not be thermodynamically interpreted. The reason to this is discussed. © 1997 Elsevier Science B.V.

Keywords: Dehydration; Fluidized bed; Process kinetics; Rare-earth chlorides

1. Introduction

Anhydrous rare-earth chlorides are compounds which are of practical use as raw materials in the metalwinning process. Neodymium metal forms an important constituent in the $Nd_2Fe_{14}B$-magnet whose share in the world market is ever growing. Terbium and dysprosium metal are important elements, for example in the 'Terfenol-D'™ alloy ($Tb_{0.27}Dy_{0.73}$ $Fe_{1.8-2.0}$) which is foreseen to be used in many future applications because of its giant magnetostrictive power.

In a previous work [1], a fluidized bed reactor was used to investigate the dehydration schemes of entitled compounds. Hydrolysis was avoided by using a dry gas flow of argon and hydrogen chloride. $NdCl_3 \cdot 6H_2O$ and $TbCl_3 \cdot 6H_2O$ were found to decompose to their anhydrous states through the reaction steps $6 \rightarrow 3 \rightarrow 2 \rightarrow 1 \rightarrow 0$; and $DyCl_3 \cdot 6H_2O$ was found to decompose through the reaction steps $6 \rightarrow 3 \rightarrow 1 \rightarrow 0$. Under constant and isothermal conditions, the specific reactions were proceeded. Reaction steps from hexahydrate to monohydrate were proceeding successively and transfer points were indicated by a sudden reduction of reaction rate. At compositions close to the monohydrated and anhydrous chloride, reaction rate was reduced abruptly and was followed by a slow convergence toward the end-products, respectively.

From kinetic theory, reactions may be considered to occur in a series of mass transfer and chemical reaction steps, which in the present situation involves at least the following:

*Corresponding author. Fax: 00 46 8 149338; e-mail: johans@metallurgi.kth.se

PII S0040-6031(97)00293-1

(I) Transport of water from the particle core of unreacted hydrate to the particle surface.
(II) Chemical reaction, involving desorption of water from the particle surface to the gas phase.
(III) Outward diffusion of water gas through the porous channels to the outer surface of the particle.
(IV) Outward diffusion of water gas through the boundary layer surrounding the particle to the bulk of the gas phase.
(V) Transport of water gas by bulk flow.

The overall reaction rate is given by the slowest step or a combination of two or more steps with comparable rates (mixed-control kinetics).

In the present work, a series of isothermal experiments have been carried out by the fluidized bed technique. The influence of different process parameters was considered in order to find out the rate determining parameters of the constant reaction rate regimes and explain the process kinetics of the fluidized bed.

2. Experimental details

2.1. Materials

Nd_2O_3, Tb_4O_7 and Dy_2O_3 of 99.9% purity were supplied by Rhône Poulenc Chimie, France. Argon of 99.996% purity (<5 ppm H_2O and <5 ppm O_2) and hydrogen chloride gas of 99.995% purity were supplied by AGA Gas, Sweden.

2.2. Equipment and procedure

Hydrochloric acid (Pro Analysi) was used to dissolve the oxides into clear solutions. In case of terbium oxide (Tb_4O_7), hydrogen peroxide (Pro Analysi) had to be added continuously during the dissolution process. Excess water was boiled off during constant stirring and hexahydrated rare-earth chlorides were precipitated until a thick slurry was obtained. After the slurry had been cooled to room temperature the excess solution was filtered off. The solid product was vacuum-treated (<1 torr) at 40°C in order to remove excess water. Grinding and stirring were conducted at intervals to finally obtain a completely dry and

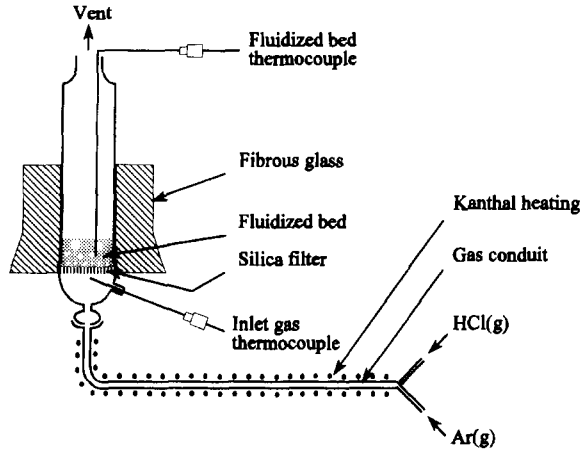

Fig. 1. Schematic picture of the experimental set-up.

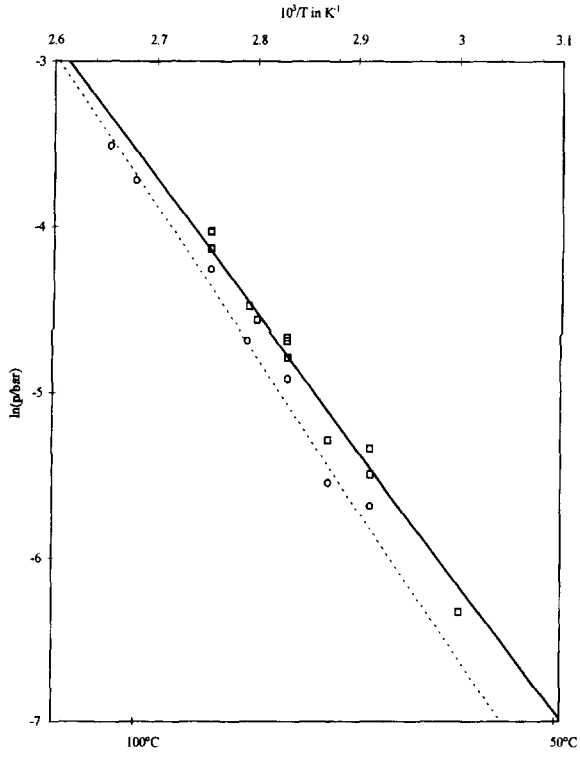

Fig. 2. Water partial pressure as a function of temperature: □, $TbCl_3{\cdot}6H_2O \rightarrow TbCl_3{\cdot}3H_2O + 3H_2O$ (this work); ○, $DyCl_3{\cdot}6H_2O \rightarrow DyCl_3{\cdot}3H_2O + 3H_2O$ (this work); ———, measured data [2] for the first reaction step of $TbCl_3{\cdot}6H_2O$; - - -, measured data [2] for the first reaction step of $DyCl_3{\cdot}6H_2O$.

Table 1
Experimental data for the dehydration of $NdCl_3 \cdot 6H_2O$

Batch	T (°C)	Δd_p (10^{-6} m)	n_{Nd} (10^{-3} mol)	G (10^{-3} mol/s)	$\dot{z}$ (10^{-6} s^{-1})	p_{H_2O} (10^{-3} bar)
$NdCl_3 \cdot 6H_2O \rightarrow NdCl_3 \cdot 3H_2O + 3H_2O$						
Nd15	55	180–250	137	7.4	477	8.75
Nd14	60	250–355	134	7.4	796	14.2
Nd16	60	180–250	121	7.4	80.3	1.31
Nd6	70	250–355	108	7.4	1399	20.0
Nd2	75	250–355	135	7.4	1456	25.9
Nd8	75	250–355	117	7.4	1612	26.1
Nd3	80	250–355	125	7.4	2535	41.1
Nd11	80	250–355	114	7.4	2288	36.4
Nd5	85	250–355	124	7.4	3256	51.7
Nd7	85	180–250	126	6.0	2713	53.9
$NdCl_3 \cdot 3H_2O \rightarrow NdCl_3 \cdot 2H_2O + H_2O$						
Nd15	60	180–250	132	7.4	53.7	0.957
Nd16	60	180–250	131	7.4	702	12.4
Nd12	65	180–250	151	6.7	91.7	2.05
Nd15	65	180–250	127	7.4	113	1.94
Nd1	70	250–355	131	7.4	199	3.51
Nd6	70	250–355	100	7.4	210	2.83
Nd2	75	250–355	131	7.4	333	5.86
Nd14	75	250–355	124	7.4	366	6.10
Nd13	80	250–355	142	7.4	1903	37.9
Nd3	80	250–355	118	7.4	427	6.76
Nd5	85	250–355	117	7.4	790	12.3
Nd13	85	250–355	134	7.5	673	11.9
$NdCl_3 \cdot 2H_2O \rightarrow NdCl_3 \cdot H_2O + H_2O$						
Nd1	70	250–355	121	7.4	26.9	0.440
Nd6	70	250–355	92	7.4	52.0	0.646
Nd2	75	250–355	124	7.4	40.5	0.678
Nd14	75	250–355	109	7.4	58.8	0.865
Nd3	80	250–355	111	7.4	105	1.57
Nd10	85	250–355	131	7.4	132	2.33
Nd5	85	250–355	108	7.4	130	1.89
Nd7	85	250–355	114	6.0	142	2.69
Nd12	90	180–250	141	6.7	239	4.98
Nd13	95	250–355	128	7.4	358	6.15
Nd15	100	180–250	120	7.4	676	10.8
$NdCl_3 \cdot H_2O \rightarrow NdCl_3 + H_2O$						
Nd12	150	180–250	127	6.9	161	2.97
Nd12	155	180–250	118	6.9	236	4.04
Nd2	160	250–355	115	7.7	363	5.39
Nd16	160	180–250	110	6.3	344	6.01
Nd31	65	250–355	99	7.7	574	7.33
Nd11	70	250–355	114	7.7	933	13.6
Nd41	70	250–355	84	7.7	820	8.87
Nd13	170	250–355	110	5.9	428	7.92
Nd15	170	180–250	113	5.9	699	13.2
Nd51	75	250–355	99	7.7	1167	14.8
Nd7	180	250–355	106	6.3	1079	17.8

sievable hexahydrated rare-earth chloride product. The powder was sieved into different fractions up to a maximum particle diameter of 425 μm. In order to remove the dusty part of the finest fraction, a pre-fluidization was executed at room-temperature. This operation ensured that less than 5% of the total bed load was carried away with the gas during the course of the experiment.

Fluidization was carried out with the equipment shown in Fig. 1. The gas-conduit and the fluidization tube were made of Pyrex glass. The fluidization tube measured 50 mm as inner diameter and 400 mm in height. The gas stream was heated before the fluidization tube by a Kanthal wire wound around the gas-conduit. The temperature was measured by Chromel-Alumel (type K) thermocouples at two positions: (1)

Table 2
Experimental data for the dehydration of $TbCl_3 \cdot 6H_2O$

Batch	T (°C)	Δd_p (10^{-6} m)	n_{Tb} (10^{-3} mol)	G (10^{-3} mol/s)	$\dot{\varepsilon}$ (10^{-6} s^{-1})	p_{H_2O} (10^{-3} bar)
$TbCl_3 \cdot 6H_2O \rightarrow TbCl_3 \cdot 3H_2O + 3H_2O$						
Tb7	60	250–355	110	9.1	148	1.78
Tb4	70	180–250	122	6.4	252	4.79
Tb13	70	150–180	112	7.4	273	4.11
Tb9	75	250–355	104	7.4	361	5.05
Tb2	80	180–250	126	7.4	542	9.16
Tb8	80	180–250	104	7.4	673	9.38
Tb14	80	150–180	130	7.4	476	8.29
Tb11	84	180–250	120	7.0	615	10.4
Tb15	85	150–180	129	7.4	658	11.3
Tb1	90	180–250	122	7.4	1098	17.8
Tb6	90	250–355	115	7.4	1041	16.0
Tb10	90	250–355	120	7.4	1110	17.7
$TbCl_3 \cdot 3H_2O \rightarrow TbCl_3 \cdot 2H_2O + H_2O$						
Tb13	70	150–180	96	7.4	112	1.45
Tb9	75	250–355	95	7.4	193	2.47
Tb8	80	180–250	80	7.4	295	3.18
Tb14	80	150–180	118	7.4	201	3.19
Tb12	85	180–250	133	7.6	266	4.63
Tb15	85	150–180	118	7.4	288	4.57
Tb1	90	180–250	114	7.4	413	6.33
$TbCl_3 \cdot 2H_2O \rightarrow TbCl_3 \cdot H_2O + H_2O$						
Tb13	70	150–180	80	7.4	45	0.486
Tb9	75	250–355	85	7.4	70	0.803
Tb14	80	150–180	108	7.4	77	1.12
Tb12	85	180–250	119	7.6	96	1.50
Tb15	85	150–180	100	7.4	99	1.34
Tb10	90	250–355	104	7.4	177	2.48
$TbCl_3 \cdot H_2O \rightarrow TbCl_3 + H_2O$						
Tb13	180	150–180	64	7.9	119	0.967
Tb3	190	250–355	98	7.5	106	1.38
Tb5	190	250–355	92	7.2	134	1.71
Tb15	195	150–180	87	7.9	246	2.71
Tb1	200	180–250	102	7.4	243	3.34
Tb2	200	180–250	94	7.2	306	3.98
Tb4	200	180–250	102	6.5	187	2.94
Tb14	205	150–180	95	7.9	398	4.78
Tb6	210	250–355	94	7.3	468	5.97

in the inlet gas stream before the silica filter and (2) in the fluidized bed. The bed temperature was controlled by a PID-regulator and the inlet gas temperature, which varied according to the heating power, was recorded continuously. In order to minimize temperature drop near the walls of the tube, the outer walls were insulated with fibrous glass. The temperature homogeneity of the bed was within ±0.2 °C. Turbulent mixing of particles and homogeneous temperature distribution were ensured by carrying out fluidization in the vigorously bubbling state, which implies that the gas-flow rate was well above the minimum fluidization value. The gas-flow rates of Ar and HCl were measured by flow meters to accuracies within ±5 and ±10%, respectively.

During fluidization, samples were taken by a small glass cup suspended from a steel wire. Samples, weighing about 400 mg, were quickly put into 15 ml jars with tightly sealed screw caps and stored in a dessicator before analysis. Samples were analyzed for chlorine by the gravimetric silver chloride method. The molar water content, z ($RCl_3 \cdot zH_2O$), was calculated from the chlorine content of the sample. The uncertainty in this method has been estimated to $\Delta z = \pm 0.002$. However, a necessary prerequisite for the precision given is that samples are free of hydrolytic compounds. Since these compounds are insoluble in water, their presence or absence was visually checked during the performance of analyses. Experiments with samples showing traces of insoluble compounds were rejected.

3. Results and discussion

Reaction rates were calculated from the linear adaptions of plotted data over the periods of constant reaction rate. The results are together with pertinent experimental data presented in Tables 1–3. Although a complete investigation of all process parameters' influence on the reaction rate was not made here, it

Table 3
Experimental data for the dehydration of $DyCl_3 \cdot 6H_2O$

Batch	T (°C)	Δd_p (10^{-6} m)	n_{Dy} (10^{-3} mol)	G (10^{-3} mol/s)	$\dot{z}$ (10^{-6} s^{-1})	p_{H_2O} (10^{-3} bar)
$DyCl_3 \cdot 6H_2O \rightarrow DyCl_3 \cdot 3H_2O + 3H_2O$						
Dy21	70	180–250	129	6.7	178	3.40
Dy11	75	<180	60	2.5	166	3.91
Dy18	80	355–425	108	15.5	1056	7.30
Dy22	85	180–250	117	6.7	532	9.16
Dy21	90	180–250	118	6.7	813	14.1
Dy26	100	250–355	134	8.9	1650	24.2
Dy25	104	<180	115	7.3	1960	29.9
$DyCl_3 \cdot 3H_2O \rightarrow DyCl_3 \cdot H_2O + 2H_2O$						
Dy20	70	355–425	88	14.2	142	0.879
Dy18	80	355–425	100	15.5	383	2.46
Dy22	85	180–250	109	6.7	258	4.16
Dy17	90	355–425	108	13.1	725	5.94
Dy21	90	180–250	110	6.7	388	6.30
Dy16	100	250–355	125	8.9	757	10.5
Dy12	110	<180	70	2.5	724	19.6
Dy15	110	<180	107	7.31	400	20.1
$DyCl_3 \cdot H_2O \rightarrow DyCl_3 + H_2O$						
Dy20	180	355–425	74	11.5	216	1.39
Dy17	190	355–425	97	13.3	370	2.69
Dy19	190	355–425	82	11.6	396	2.79
Dy4	200	<180	48	2.6	250	4.67
Dy14	210	250–355	118	8.8	517	6.86
Dy16	210	250–355	105	7.3	523	7.49
Dy10	220	<180	91	2.6	328	11.3

was already at an early stage observed that the use of different particle fractions had no decisive influence on the overall reaction rate. However, the gas-flow rate seemed to have a strong influence (see Table 3). This behaviour might be consistent with reaction rate controlled by the transport of water gas by bulk flow (step V above). In order to further investigate this hypothesis, the water partial pressure of gas leaving the bed (p_{H_2O}) was estimated by the following molar balance: rate of water entering the bed atmosphere by dehydration = rate of water exiting the bed atmosphere by gas flow. By mathematical formulation the expression becomes:

$$n_R \dot{z} = \frac{p_{H_2O}}{p_{TOT} - p_{H_2O}} G \qquad (1)$$

p_{TOT} represents the total gas pressure in the fluidized bed, G the molar flow rate of inlet gas, n_R the rare-earth molar bed load and $\dot{z}$ the reaction rate. The results of the thereby calculated p_{H_2O}-data are included in Tables 1–3.

Table 4
Standard reaction enthalpies (kJ/mol) of the reaction $RCl_3 \cdot 6H_2O \rightarrow RCl_3 + 6H_2O(g)$

R	Calorimetrically deduced data [3,4]	This work
Nd	383	467
Tb	411	491
Dy	419	475

Ukraintseva et al. [2] measured equilibrium vapour pressures over the first reaction step of $TbCl_3 \cdot 6H_2O$ and $DyCl_3 \cdot 6H_2O$ by autogeneous dehydration using a membrane pressure device. In Fig. 2 they are com-

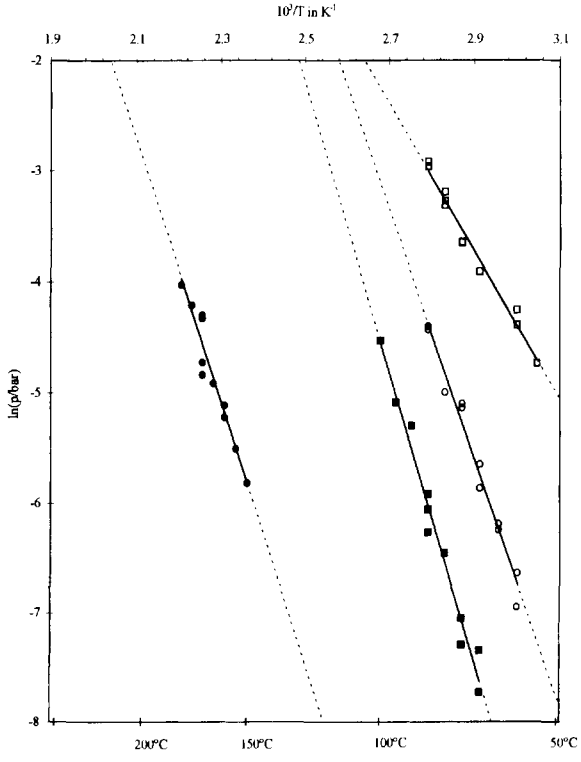

Fig. 3. Water partial pressure as a function of temperature. □, $NdCl_3 \cdot 6H_2O \rightarrow NdCl_3 \cdot 3H_2O + 3H_2O$; ○, $NdCl_3 \cdot 3H_2O \rightarrow NdCl_3 \cdot 2H_2O + H_2O$; ■, $NdCl_3 \cdot 2H_2O \rightarrow NdCl_3 \cdot H_2O + H_2O$; ●, $NdCl_3 \cdot H_2O \rightarrow NdCl_3 + H_2O$; ———, linear adaption; - - -, extrapolation.

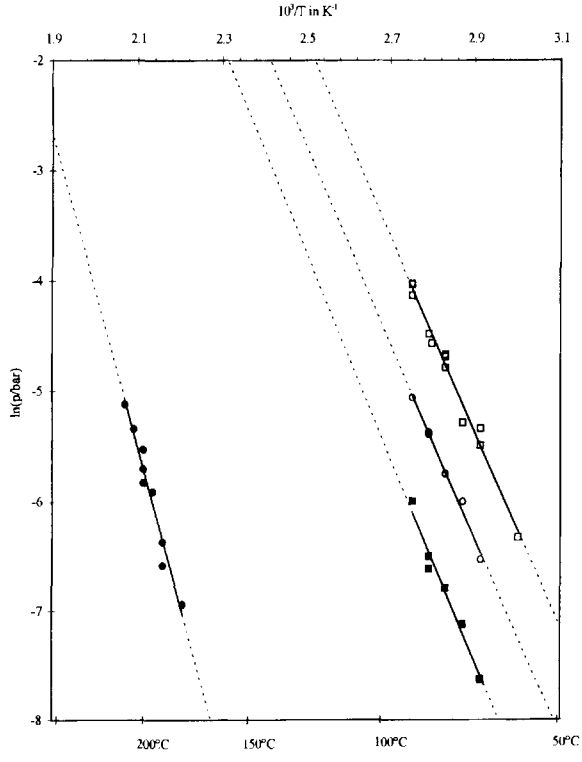

Fig. 4. Water partial pressure as a function of temperature. □, $TbCl_3 \cdot 6H_2O \rightarrow TbCl_3 \cdot 3H_2O + 3H_2O$; ○, $TbCl_3 \cdot 3H_2O \rightarrow TbCl_3 \cdot 2H_2O + H_2O$; ■, $TbCl_3 \cdot 2H_2O \rightarrow TbCl_3 \cdot H_2O + H_2O$; ●, $TbCl_3 \cdot H_2O \rightarrow TbCl_3 + H_2O$; ———, linear adaption; - - -, extrapolation.

pared with the present results of reactions 6 → 3. As can be seen, the agreement is very good and it might be concluded that the flow of gas leaving the fluidized bed is close to equilibrium with respect to water vapour, thereby supporting the previously submitted hypothesis. Figs. 3–5 show all the estimated water partial pressures based on the tabulated results as a function of temperature. Linear adaptions of the specific reactions have been made, which show that the data are possible to implement into equilibrium relationships. Consequently, another assessment of the estimated data may be done by calculating the standard reaction enthalpies according to the Clausius–Clapeyron equation:

$$\Delta H^0 = -\upsilon R \frac{\Delta \ln p_{H_2O}}{\Delta(1/T)} \quad (2)$$

where υ represents the moles of water lost per mole of reaction, R the gas constant and the quotient represents the slope of the linear adaptions. The calculated results are summed up to the enthalpy of reaction 6 → 0 and compared with calorimetrically deduced data [3,4] in Table 4. On comparing, the values of Table 4 are in poor agreement; standard reaction enthalpies of this work apparently exceed the calorimetrically deduced data by 13 to 22%. In view of the previous comparisons made in Fig. 2, these disagreements are surprising, since it would imply that the technique of equilibration by autogeneous dehydration [2] does not result in true equilibrium values. Andersson et al. [5] concluded that isothermal systems of hydrated salts are not likely to attain true chemical equilibrium by autogeneous reaction, because reactions apparently cease to occur during a certain range of p_{H_2O} (see Fig. 6). They demonstrated the existence of an inhibition domain around the equilibrium line of a hydrated salt system, see Fig. 7. $\ln(p_{H_2O}) - 1/T$ lines, delimiting the inhibition domain, constitute the dynamic limits for dehydration/hydration and hinder reactions to proceed in a further approach to equilibrium. Accordingly, all the results presented in Figs. 2–5 are more likely to represent the dynamic limits of dehydration instead of true equilibrium lines. This is further on substantiated by the factual difference in slopes of the limiting dehydration line and the equlibrium line in Fig. 7, being in accordance with the calorimetric comparisons shown in Table 4.

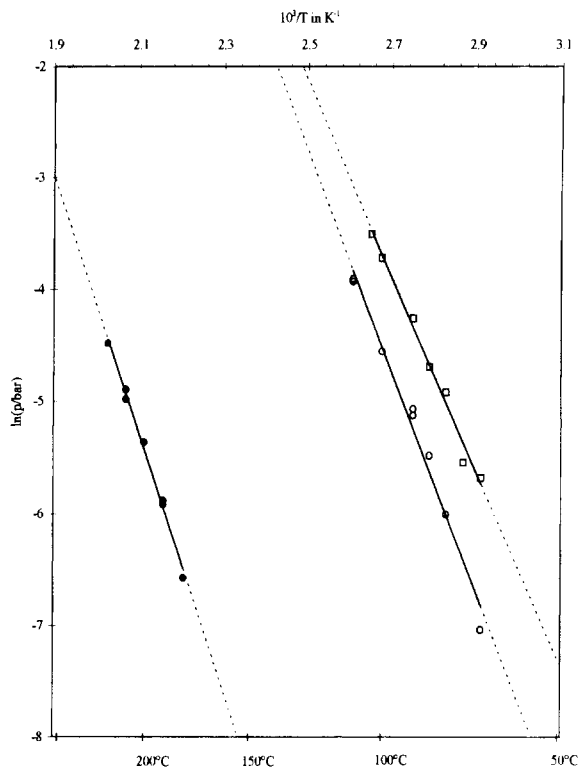

Fig. 5. Water partial pressure as a function of temperature. □, $DyCl_3 \cdot 6H_2O \rightarrow DyCl_3 \cdot 3H_2O + 3H_2O$; ○, $DyCl_3 \cdot 3H_2O \rightarrow DyCl_3 \cdot H_2O + 2H_2O$; ●, $DyCl_3 \cdot H_2O \rightarrow DyCl_3 + H_2O$; ———, linear adaption; - - -, extrapolation.

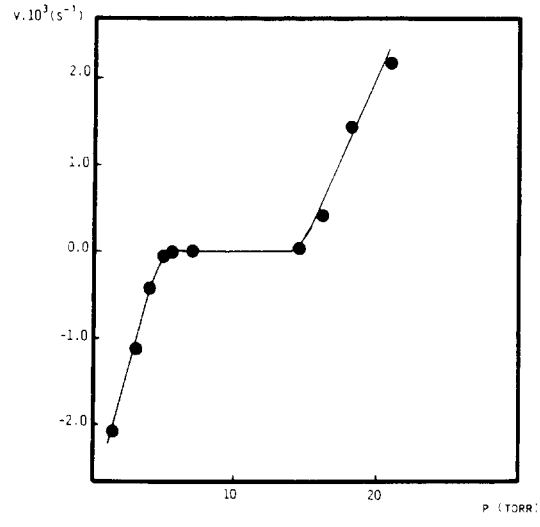

Fig. 6. Reaction rate vs p_{H_2O} for a mixture of $MgCl_2 \cdot 6H_2O$ and $MgCl_2 \cdot 4H_2O$. (Andersson et al. [5])

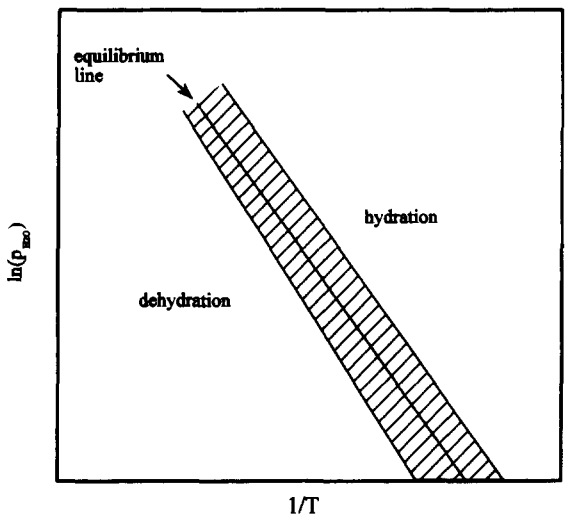

Fig. 7. A typical pressure-temperature diagram for a salt hydrate system exhibiting a large extent of inhibition (hatched area) around the equilibrium line. The pressure-temperature lines, delimiting the inhibition domain, constitute the dynamic limits for dehydration- and hydration reactions, respectively. (Andersson et al. [5])

Thus, the kinetic behaviour of the fluidized bed dehydration is best described as being limited by a 'saturated' bulk gas flow rather than 'equilibrated'. The estimated saturation values are useful from an engineering point of view, since they can be used to predict the overall reaction rate of the dehydration process.

4. Conclusions

The overall kinetics of the fluidized bed process for the dehydration of $NdCl_3 \cdot 6H_2O$, $TbCl_3 \cdot 6H_2O$ and $DyCl_3 \cdot 6H_2O$ have been considered. A comparison between estimated vapour pressures of gas leaving the bed and corresponding data from gas phase equilibration of $TbCl_3 \cdot 6H_2O$ and $DyCl_3 \cdot 6H_2O$ by autogeneous dehydration [2] were in accordance, thus it may be concluded that dehydration in the fluidized bed attains a saturation state in close approach to equilibrium with respect to the gas phase leaving the bed. In kinetic terms this may be interpreted as the overall reaction rate is controlled by the transport of water gas by bulk flow rate of a saturated gas phase. Based on the linear relations of $\ln(p_{H_2O})$ versus $1/T$, this behaviour seems to be consistent for all reactions and conditions studied in the present experimental work. However, comparisons between estimated enthalpies from the slopes and calorimetric data from literature show a systematic discrepancy from true equilibrium behaviour. This has been explained by the existence of an inhibition domain around equilibrium which hinder the reactions to attain equilibrium [5]. Therefore, estimated as well as measured water vapour pressures [2] from autogeneous dehydration might not be suitable to use for thermodynamic calculations. Instead, they seem to represent the practical saturation state of the reaction in an isothermal system.

5. List of symbols and units

Δd_p	particle fraction, m
G	inlet gas-flow rate, mol s^{-1}
ΔH	reaction enthalpy, J mol^{-1}
n_R	molar bed load, mol
p_i	partial pressure, bar or (bar/1 bar)
R	gas constant, J K^{-1} mol^{-1}
T	temperature, °C or K
z	water molar content (moles H_2O/mole RCl_3), -
$\dot{z}$	reaction rate of dehydration $(-dz/dt)$, s^{-1}
υ	stoichiometric constant, -

Acknowledgements

The present work has been carried out by the financial aid of NUTEK (National Board for Industrial and Technical Development).

References

[1] J. Sundström and O. Wijk, Investigation of the dehydration schemes of $NdCl_3 \cdot 6H_2O$, $TbCl_3 \cdot 6H_2O$ and $DyCl_3 \cdot 6H_2O$ using a fluidized bed (Paper presented at the 21st Rare Earth Research Conference, Duluth - Minnesota, July 7–12 1996).

[2] É. Ukraintseva, A.N.P. Sokolova, V.A. Logvinenko, Soviet Radiochemistry 31 (1989) 4.
[3] F.H. Spedding, J.A. Rard, A. Habenschuss, J. Phys. Chem. 81 (1977) 1069.
[4] D.D. Wagman, W.H. Evans, V.B. Parker, R.H. Schumm, I. Halow, S.M. Bailey, K.L. Churney and R.L. Nuttall: The NBS tables of chemical thermodynamic properties in J. Phys. Chem. Ref. Data, 11 (1982) suppl. no. 2.
[5] J. Andersson, M. Azoulay, J. De Pablo, Int. J. Energy Res. 12 (1988) 137.